Automatic segmentation and classification of ESF patterns using a U-NET-based model

EQIT-4

2024

Susan Palacios and Marco Milla

Pontificia Universidad Católica Del Perú

e-mail: spalacios@pucp.edu.pe

Abstract

Equatorial Spread F (ESF) is a phenomenon that occurs in the magnetic equatorial ionosphere and can disturb radio signal propagation at night. This phenomenon is caused by depleted areas of plasma density (also known as bubbles) that begin at the bottom of the ionospheric F region. The Jicamarca Radio Observatory (JRO) in Peru has made it possible to study ESF using the 50 MHz Jicamarca ionospheric radar in the low-power mode called JULIA (Jicamarca Unattended Long-Term Studies of the Ionosphere and Atmosphere). The radar detects backscattered signals caused by the ESF structures, generating Range-Time-Intensity (RTI) power maps that show the temporal and spatial (altitude) occurrence of ESF. The Madrigal database contains over 20 years of RTI maps measured at Jicamarca, allowing us to identify different ESF morphological patterns or structures [1,2,3], such as Bottom-type, Bottomside, and Radar plumes. These patterns show the evolution of the ESF and can be used to forecast it. However, manually identifying these structures is a time-consuming process. To overcome this issue, a deep learning model using the U-Net convolutional neural network architecture was implemented to segment and classify four morphological patterns automatically. The model was trained using various features such as backscatter power, the F10.7 solar flux index, the disturbance storm time index, the Moon phase, the vertical drift, the zonal drift, and the statistical texture information of backscatter power and vertical drift. The proposed model achieved an accuracy of 90.01% in segmenting and classifying the structures. This model was applied to the RTI database, allowing us to obtain climatology statistics for each morphological pattern.

Data

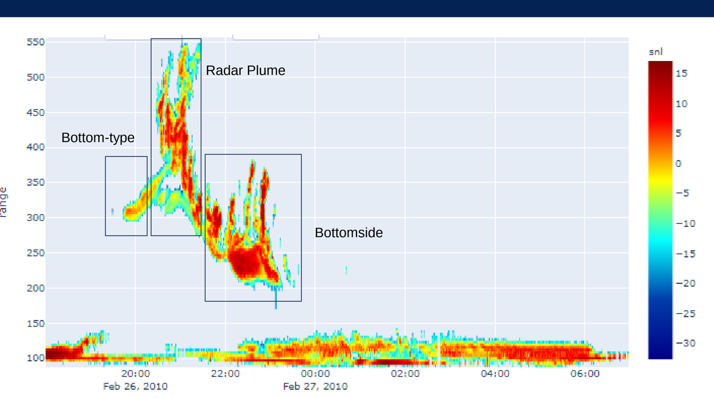

Figure 1: RTI map of echoes measured by JULIA on 26 February 2010.

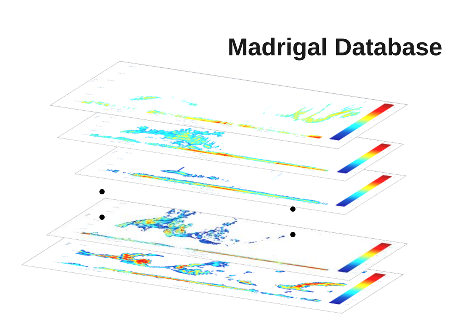

Figure 2: 2930 RTIs maps corresponding to the years 1999 and 2022.

Building training data

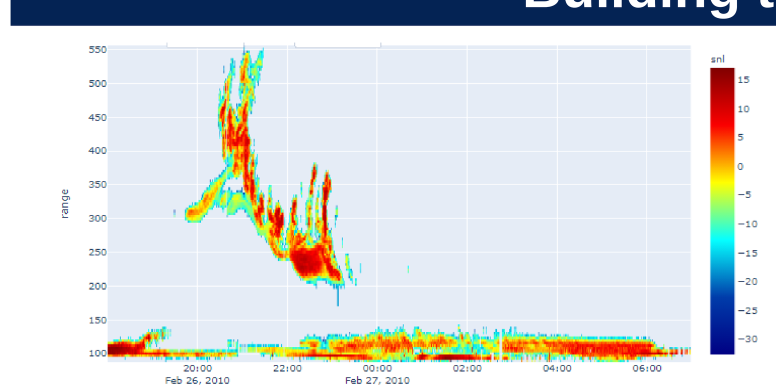

Figure 3: RTI map showing the backscatter power.

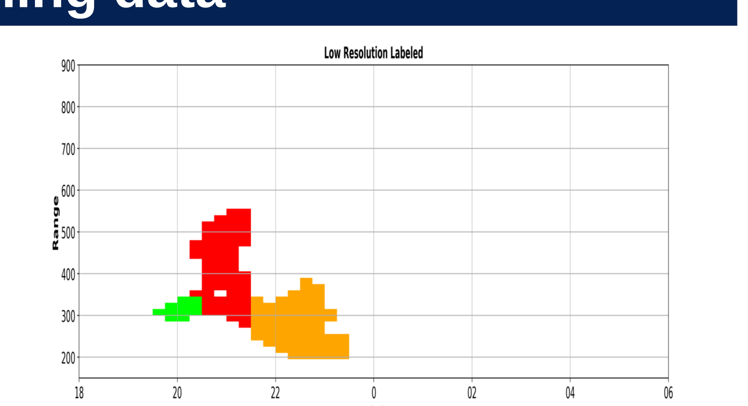

Figure 6: Low resolution segmented RTI map (15 min by 15 km) [4].

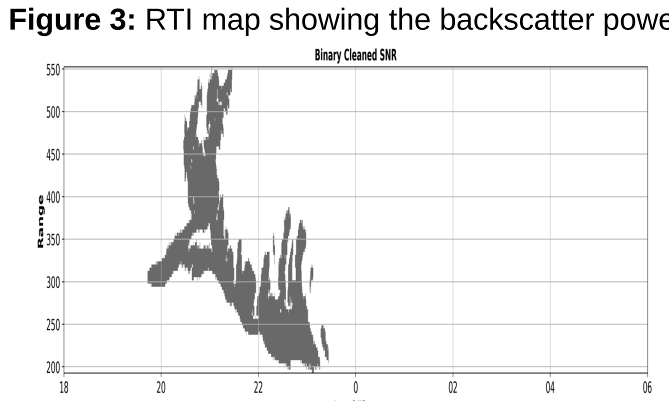

Figure 4: Binary RTI map, after removing small artifacts.

Using the SNR, physical parameters and statistical textures we built feature bands.

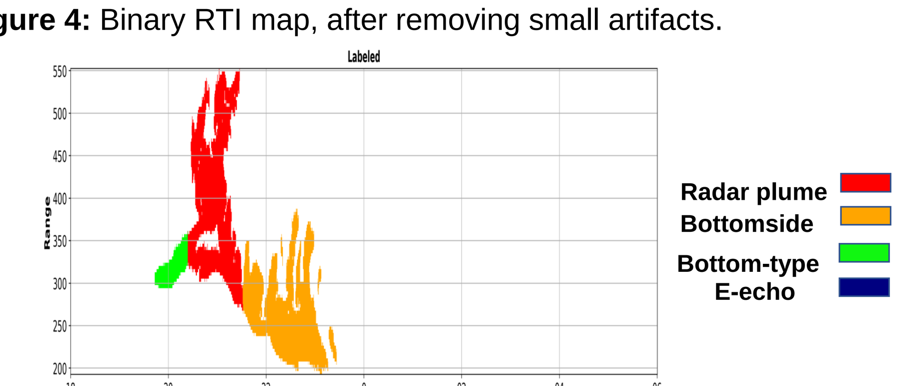

Figure 5: Manually identification using four classes (Bottom-type, Bottom-side, Radar plumes, and E-echoes)

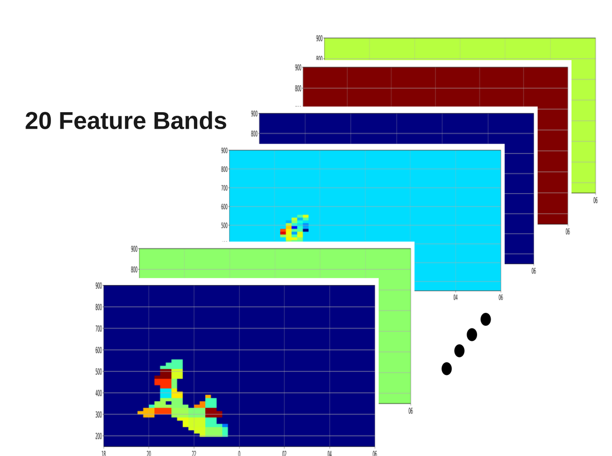

Figure 7: Stack of SNR, Zonal Drift, Vertical Drift, F10.7, DST, DOY, lunar phase, SNR, and vertical drift statistical textures(Mean intensity, Contrast, Uniformity, Entropy, Smooth, Third Moment).

Training model

For training, validation, and testing the model, we used 539 RTI maps. The validation data set allowed us to observe the model performance during the hyperparameters tuning. While the testing gives us the model performance in unseen data.

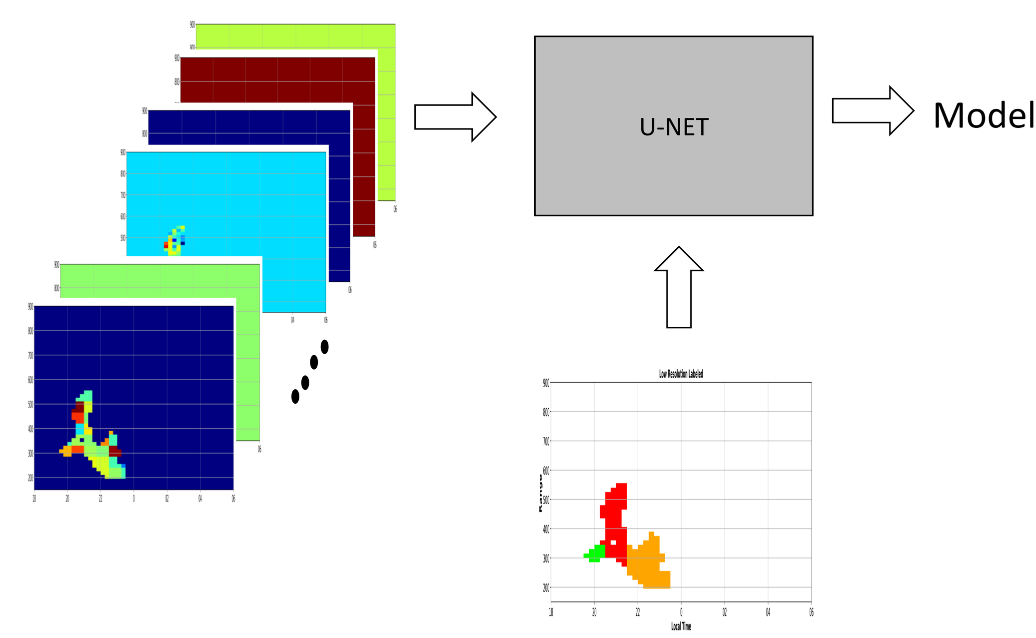

Figure 8: Training the model with the feature stack and the low resolution labeled RTI map.

Table 1: Data Set Size.

Data Set	N. Of RTI maps
Train	391 (73%)
Validation	98 (18%)
Test	50 (9%)

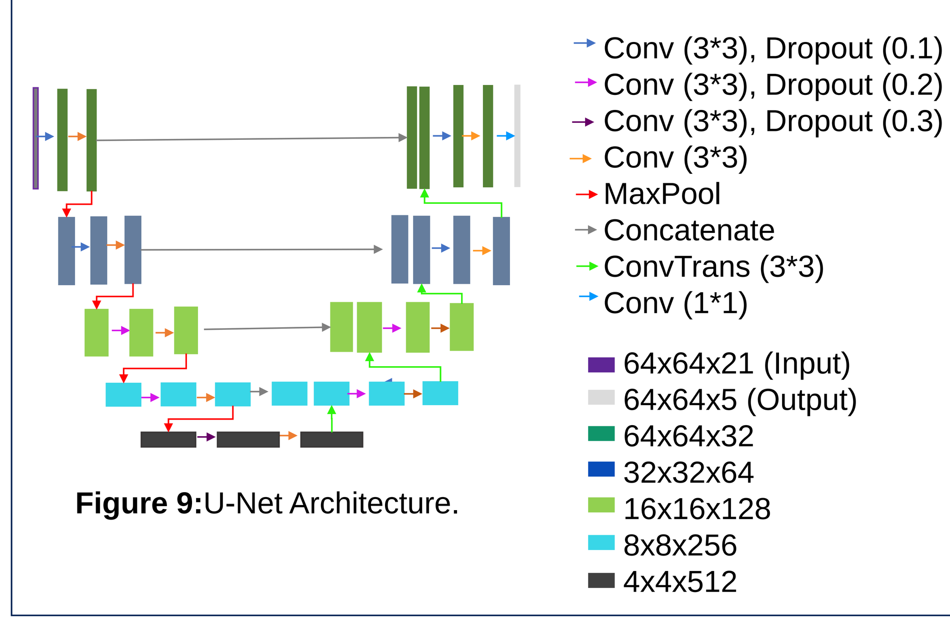

Figure 9: U-Net Architecture.

Table 2: Model configuration.

UNET
• Learning rate: 0.001
• Optimizer: Adam,
• Activation: RELU.
• Loss function: Categorical Cross entropy.
• Number of epoch: 42
• Batch size:32
• Filter size: 3x3
• Dropout rate:0.1,0.2,0.3
• Padding: Same
• Kernel Initializer: He normal, Glorot normal

Discussions and Conclusions

- Manually identifying morphological patterns is a challenging visual task. This drove the development of an automatic segmentation model based on the UNET convolutional neural network.
- Our proposed approach involves choosing the most suitable features and training a convolutional neural network architecture that helps our algorithm achieve good performance (90.01%) in segmenting the morphological patterns in RTI maps.
- Applying our methodology to the Jicamarca database, we can analyze the occurrence of each morphological pattern during each season (Solstice and Equinox) and during the solar cycle. Moreover, we can automatically get reports (start and end time, max and min range) for each morphological pattern.

References

[1] Hysell, D. L., & Burcham, J. D. (1998). JULIA radar studies of equatorial spread F. Journal of Geophysical Research, 103(A12), 29,155– 29,167. https://doi.org/10.1029/98JA02655.

[2] Hysell, D. L. (2000). An overview and synthesis of plasma irregularities in equatorial spread F. Journal of Atmospheric and Solar-Terrestrial Physics, 62 (12), 1037-1056. https://doi.org/10.1016/S1364-6826(00)00095-X

[3] Hysell, D. L., & Burcham, J. D. (2002). Long term studies of equatorial spread F using the JULIA radar at Jicamarca. Journal of Atmospheric and Solar-Terrestrial Physics, 64 (12-14), 1531-1543. https://doi.org/10.1016/S1364-6826(02)00091-3

[4] Zhan, W., F. S. Rodrigues, and M. A. Milla. 2018. "On the Genesis of Postmidnight Equatorial Spread F: Results for the American/ Peruvian Sector." Geophysical Research Letters 45(15): 7354-7361, https://doi.org/10.1029/2018GL078822

Acknowledgements

- The authors thank to CEDAR 2024 Science Steering Committee for kindly support the presentation of this work.
- We gratefully thanks the Jicamarca Radio Observatory (JRO). The JRO is a facility of the Instituto Geofísico del Perú operated with support from the NSF Award 1732209 through Cornell University.

Results

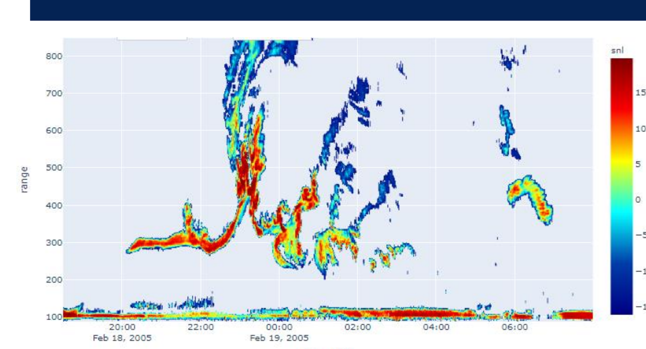

Figure 10: RTI map measured on 18 Feb 2005.

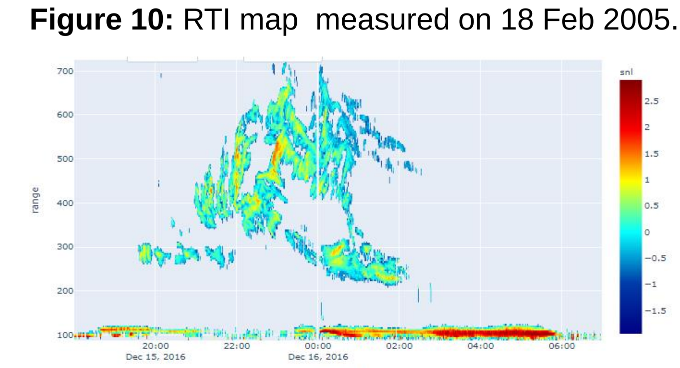

Figure 11: RTI map measured on 15 Dec 2012.

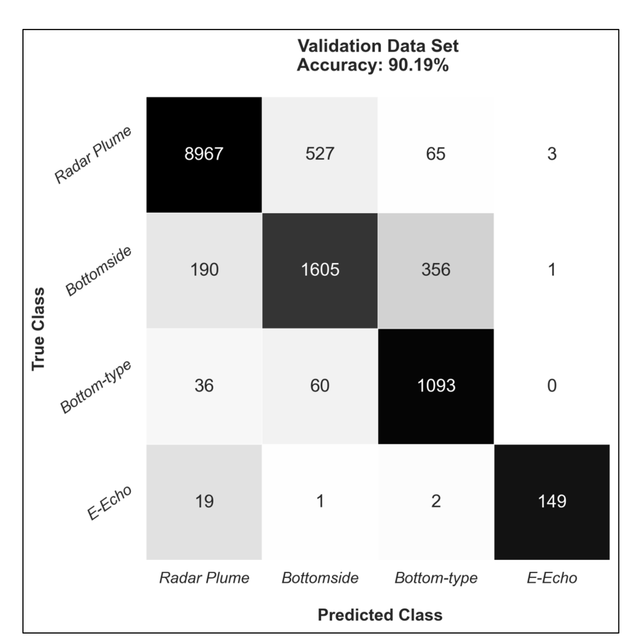

Figure 12: Confusion Matrix and accuracy using 98 RTIs.

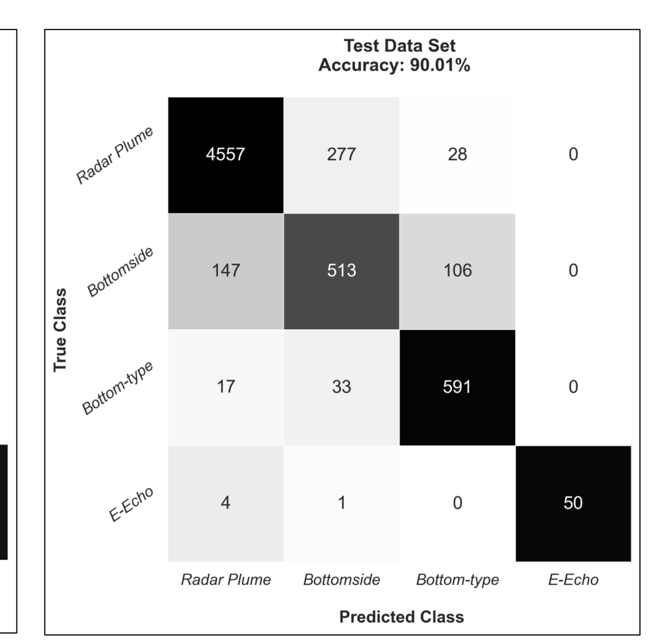

Figure 13: Confusion Matrix and accuracy using 50 RTIs.

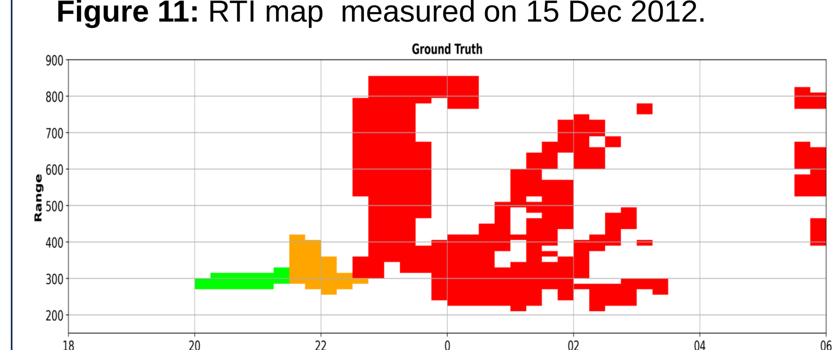

Figure 14: Figure 10 labeled manually.

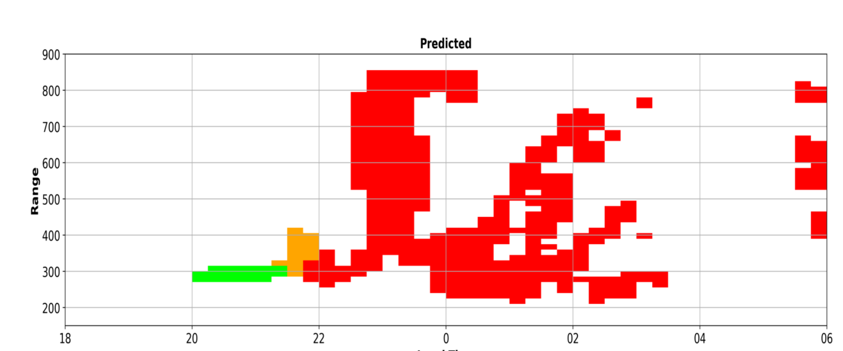

Figure 15: Predicted Segmentation (Accuracy=96.61 %) .

Radar plume
Bottomside
Bottom-type
E-echo

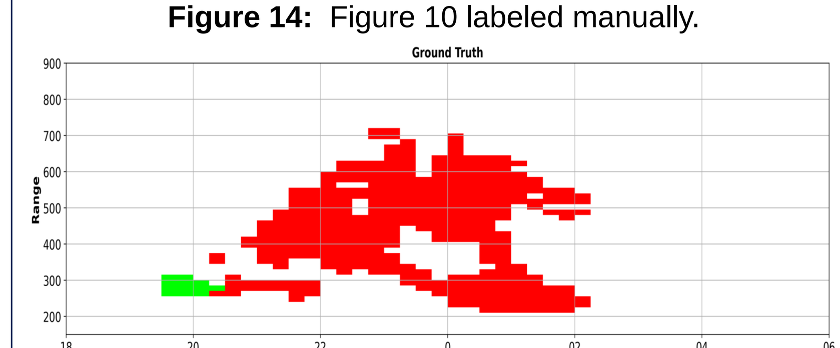

Figure 16: Figure 11 labeled manually.

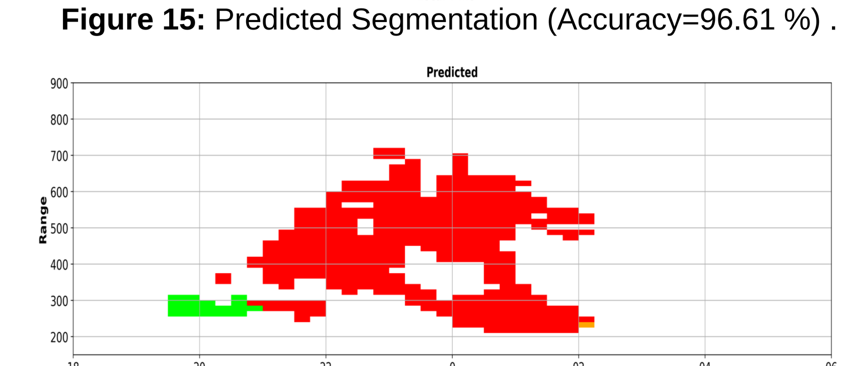

Figure 17: Predicted Segmentation (Accuracy=98.20%) .

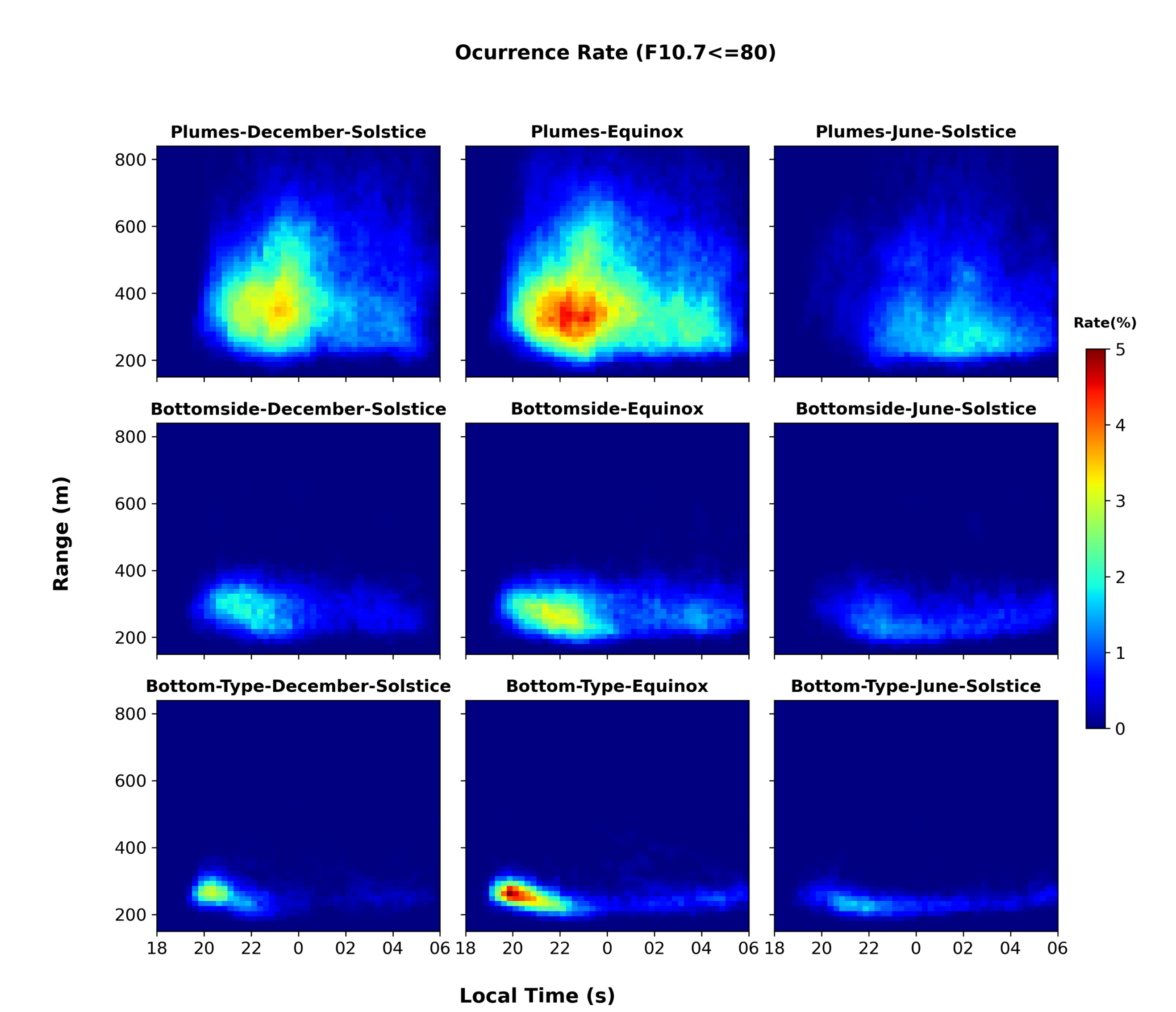

Figure 18: Occurrence Rate maps of each morphological pattern for each season during Solar Minimum and Quiet Days (kp<4). The occurrence maps were obtained after we applied the UNET model on the Jicamarca database (2930 RTIs).